JOURNAL OF GEOPHYSICAL RESEARCH, VOL. 106, NO. D3, PAGES 3057–3069, FEBRUARY 16, 2001

Measuring system for the long-term monitoring of biosphere/atmosphere exchange of carbon dioxide

L. Haszpra,[1] Z. Barcza,[2] P. S. Bakwin,[3] B. W. Berger,[4] K. J. Davis,[4] and T. Weidinger[2]

Abstract. We describe an ongoing program being carried out in Hungary to investigate the role of the temperate continental region in the global carbon cycle. Carbon dioxide mixing ratios are continuously monitored at 10, 48, 82, and 115 m above the ground on a television transmitter tower, and the atmosphere/surface exchange of CO_2 is measured by eddy covariance at 82 m. The region surrounding the tower is typical of rural areas of central Europe, with agricultural fields, forest patches, and small villages. We first describe the layout and the operation of the measuring system designed for the continuous, unattended monitoring of the vertical distribution of CO_2 mixing ratio in the lowest 115 m of the atmosphere based on a Li-Cor model 6251 infrared gas analyzer (IRGA). It provides vertical profile data with a temporal resolution of 8 min. Next, we discuss the measuring system for long-term, continuous monitoring of the biosphere/atmosphere exchange of CO_2. The eddy correlation system is based on a Li-Cor model 6262 fast-response IRGA and a Gill ultrasonic anemometer running at 4 Hz sampling frequency. Results are to illustrate the performance of the systems. Among others, they show the occasional accumulation of CO_2 in the boundary layer in the Carpathian Basin during winter and the diurnal variation of the vertical distribution of CO_2 mixing ratio in summer. A simple method based on similarity theory to calculate vertical fluxes from vertical gradients is presented, which can be used to fill the data gaps that inevitably occur during long-term eddy correlation measurements. The present study confirms the feasibility of the long-term tall-tower CO_2 flux and mixing ratio measurements.

1. Introduction

The atmospheric mixing ratio of carbon dioxide has been increasing since the Industrial Revolution as a result of human activity (see the ice core records of, e.g., *Barnola et al.* [1995] and *Etheridge et al.* [1996] and the direct atmospheric measurements reported to the World Data Center for Greenhouse Gases, World Meteorological Organization, at http://jcdc.kishou.go.jp /wdcgg.html or to the Carbon Dioxide Information Analysis Center, Oak Ridge National Laboratory, at http://cdiac.esd.ornl.gov). This increase may enhance the greenhouse effect of the atmosphere, generating global climate change [*Trenberth et al.*, 1996].

During the last decade several papers based on measurements and model calculations [e.g., *Keeling et al.*, 1989; *Tans et al.*, 1989, 1990; *Enting and Mansbridge,* 1991; *Musselman and Fox,* 1991; *Tans,* 1991; *Quay et al.*, 1992; *Sarmiento and Sundquist,* 1992; *Siegenthaler and Sarmiento,* 1993; *Sundquist,* 1993; *Conway et al.*, 1994; *Dixon et al.*, 1994; *Hesshaimer et al.*, 1994; *Ciais et al.*, 1995a,b; *Denning et al.*, 1995; *Keeling et al.*, 1996; *Taguchi,* 1996] concluded that there must be a large CO_2 sink in the Northern Hemisphere to balance the observed global carbon budget. Several lines of evidence indicate that a significant fraction of this CO_2 sink must be to the terrestrial biosphere in the northern temperate latitudes. Additional measurements are needed in continental regions to characterize the terrestrial sink and to understand the processes that control its magnitude [*Tans et al.*, 1996]. Continuous, long-term monitoring of CO_2 mixing ratios is needed at representative continental sites [e.g., *Bakwin et al.*, 1995, 1998]. Also, long-term measurements of the biosphere/atmosphere exchange of CO_2 are needed for a variety of ecosystems in a wide range of climate zones

[1]Institute for Atmospheric Physics, Hungarian Meteorological Service, Budapest, Hungary.

[2]Department of Meteorology, Eötvös Loránd University, Budapest, Hungary.

[3]Climate Monitoring and Diagnostics Laboratory, NOAA, Boulder, Colorado.

[4]Department of Soil, Water and Climate, University of Minnesota, St. Paul.

Paper number 2000JD900600.
0148-0227/01/2000JD900600$09.00

[*Baldocchi et al.,* 1996]. Our program encompasses both of these types of measurements.

Hungary is located in the northern temperate zone, in the middle of the European continent. The region has undergone intensive human management for hundreds of years. Our project was initiated as a cooperative U.S.-Hungarian scientific effort to establish a long-term monitoring site in Hungary. As the main purpose of the study is to obtain regionally representative mixing ratio and flux data, we sought an existing tall tower located as far as possible from direct anthropogenic sources. The limited budget for the project forced us to design a measurement system with a low cost and which would require minimal maintenance. In many cases we used homemade components to achieve the lowest cost while preserving the level of performance possible with commercially available equipment.

The purpose of this paper is to describe the measurement systems for CO_2 mixing ratio profiles and atmosphere/surface exchange and to illustrate the measurements with a few examples. Attention is paid to the usefulness of parallel eddy correlation and vertical profile measurements. Detailed discussion and interpretation of the data will be published in separate papers [e.g., *Haszpra,* 1999].

2. Experimental Design

2.1. Monitoring Site

The measurements were carried out on a 117-m-tall, free-standing TV and radio transmitter tower owned by Antenna Hungária Corporation. The lower 56 m is a 7.75 m diameter cylinder made of reinforced concrete, while the upper 61 m is a steel cylinder of 1.82 m diameter. As shown in Figure 1, the tower is located in a flat region of western Hungary (46°57'N, 16°39'E), at an altitude of 248 m above sea level. Figure 2 shows the surrounding land use and vegetation types. The tower is surrounded by agricultural fields (mostly crops and fodder of annually changing types) and forest patches. The distribution of vegetation types [60% arable land, 30% forest and woodland, 10% other (vineyard, settlements, etc.)] within 10 km of the tower is not greatly different from the average for the western Hungarian landscape unit (7300 km^2) or the whole country (93,000 km^2) (85% of the area is cultivated, 77% of which is agricultural and 23% of which is forest). The soil type in the region of the tower is "lessivated brown forest soil" (Alfisol, according to the U. S. Department of Agriculture system). These soils have clay migration and moderate acidity as well as a more widespread humification, leaching, and clay formation [*Stefanovits,* 1971]. The upper layer is generally 10-20 cm thick, and its organic matter content is 5-8%.

Human habitation within 10 km of the tower is only in small villages (100-400 inhabitants). The nearest village is Hegyhátsál (170 inhabitants), ~1 km to the northwest. There is no notable industrial activity in this dominantly agricultural region. Local roads have mostly low levels of traffic. One of the few main roads of the region, which carries 3600 vehicles per day on average, passes ~400 m to the southwest of the tower.

Measurements of CO_2 mixing ratio profiles, temperature, humidity, and wind profiles began in September 1994. Flux measurements began in April 1997. The tower is also a National Oceanic and Atmospheric Ad-

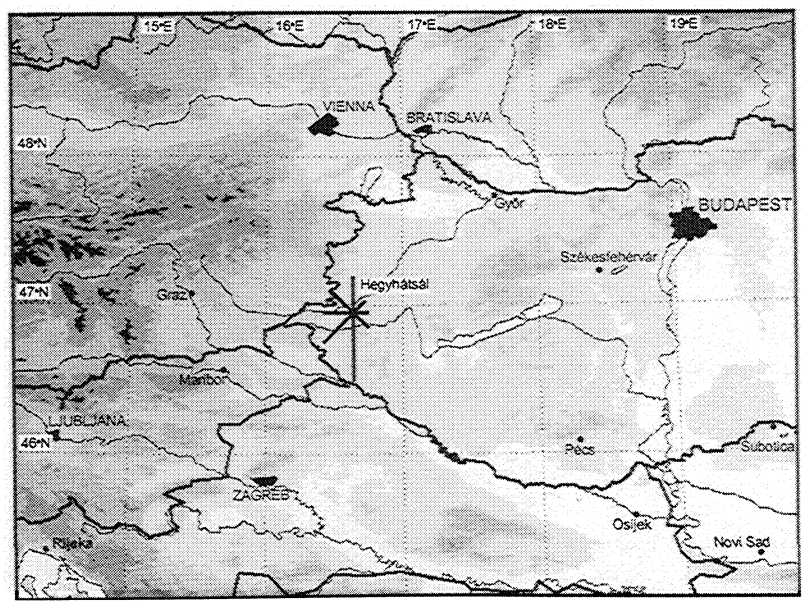

Figure 1. Shaded relief map showing the geographical location of Hegyhátsál, Hungary, and the major cities (more than 100,000 inhabitants) as well as the frequency distribution of the wind direction at Hegyhátsál. Higher altitudes appear as darker colors.

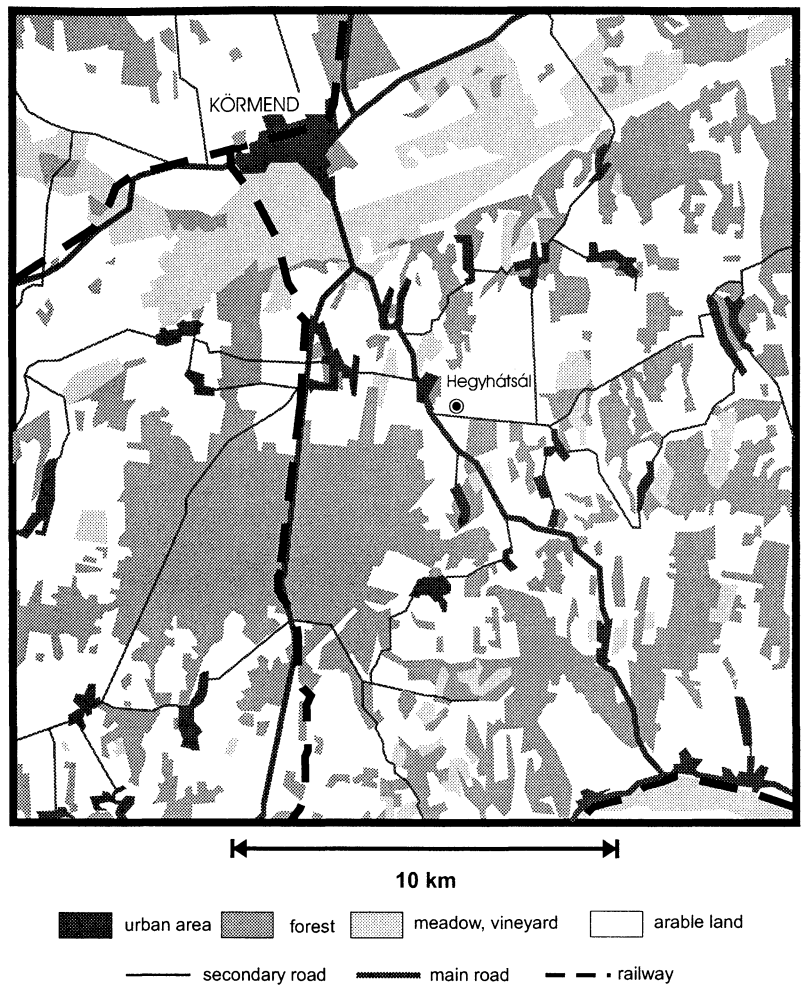

Figure 2. Land use and vegetation type distribution in the region of Hegyhátsál.

ministration (NOAA) Climate Monitoring and Diagnostics Laboratory (CMDL) global air sampling network site (site code HUN) [*Conway et al.*, 1994]. Air is sampled once per week using glass flasks, and the samples are analyzed at CMDL for CO_2, CH_4, CO, H_2, N_2O, and SF_6 and at the Institute for Arctic and Alpine Research of the University of Colorado for the stable isotopes of C and O in CO_2 (^{13}C and ^{18}O) [see *Trolier et al.*, 1996].

2.2. Measuring System for the CO_2 Mixing Ratio Vertical Profile

A schematic diagram of the CO_2 mixing ratio profile system is shown in Figure 3. Mixing ratios of CO_2 are measured at 10, 48, 82, and 115 m above the ground. Air is pumped through 9.5-mm-diameter tubes (Dekoron type 1300) to a CO_2 analyzer located in the TV transmitter building. A 47-mm-diameter (Whatman EPM) particle filter is located at the inlet of each tube. The setup for CO_2 analysis is very similar to that described by *Zhao et al.* [1997a], which was used for the measurements reported by *Bakwin et al.* [1995, 1998]. Diaphragm pumps (KNF Neuberger type UN73MVP) are used to draw air continuously through each of the tubes from the four monitoring levels at a flow rate of ~2 L/min. After leaving the pump, the air at 40 kPa overpressure enters a glass trap for liquid water that is cooled in a regular household refrigerator, to dry the air to a dew point of 3°-4°C. Liquid water is forced out through an orifice at the bottom of each trap.

The four inlet tubes and the standard gases are connected to a computer-controlled, 16-position valve (VICI AG, Valco Europe), which selects which monitoring level or standard gas is sampled by the analyzer. The valve head is protected by 7-μm in-line filters. Ambient air flows continuously through the multiport valve so that the system is constantly flushed. The (expensive) standard gases are shut off when not in use by means of computer-controlled solenoid valves. The air leaving the multiport valve through its common outlet is further dried to a dew point of about -25°C by passage through a 182-cm-long Nafion drier (Permapure, type MD-110-72P), so that the water vapor interference and dilution effect are <0.1 ppm equivalent CO_2 [*Zhao et al.*, 1997a]. The Nafion drier is purged in a counterflow (100 cm^3/min) arrangement using waste sample air that has been further dried by passage through anhydrous $CaSO_4$.

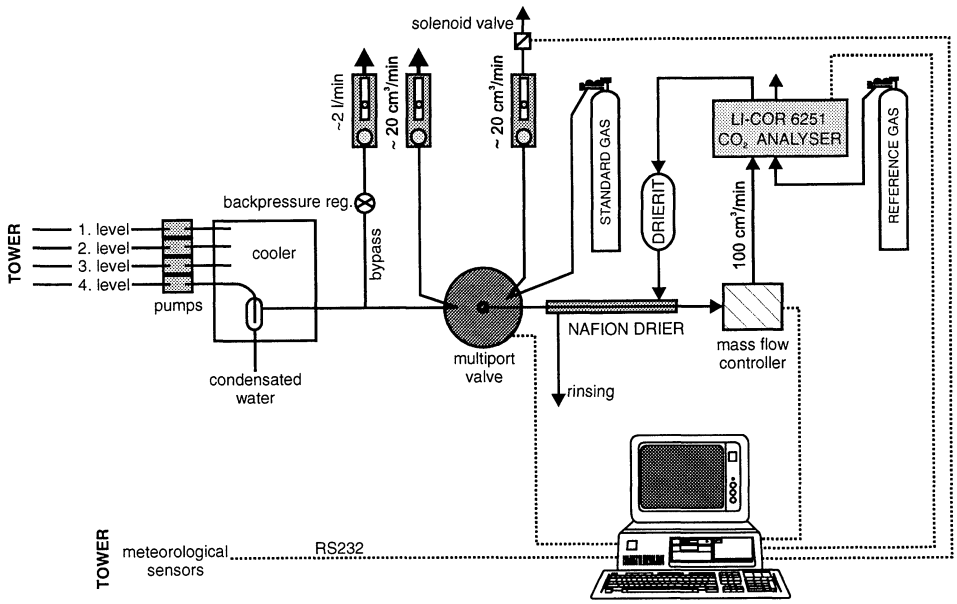

Figure 3. Layout of the monitoring system for the vertical CO_2 mixing ratio profile.

Analysis for CO_2 is carried out using an infrared gas analyzer (IRGA) (Li-Cor Inc. model LI-6251). A constant sample flow rate of 100 cm^3/min is maintained by a mass flow controller (Tylan model FC-260). The reference cell of the CO_2 analyzer is continuously flushed at a flow rate of 5-10 cm^3/min with a compressed reference gas of 330-340 ppm CO_2 in synthetic air (Messer Hungarogáz). Calibration of the analyzer is carried out using four standards spanning 330-420 ppm CO_2, which were prepared by CMDL [*Kitzis and Zhao,* 1999].

The basic measuring cycle is 2 min, consisting of 1 min flushing and 1 min signal integration. Each 1-min average and standard deviation is based on six to seven measurements. The multiport valve steps through the four monitoring levels in 8 min. Every 32 min, after four 8-min measuring cycles, the standard gas with the lowest CO_2 mixing ratio is selected and analyzed; we term this measurement a "zero". After every sixth cycle (every 202 min) a full four-point calibration is carried out. The reference and sample cells of the CO_2 analyzer are not pressure or temperature controlled. The zero measurements are used to account for any short-term drift of the analyzer due to changes in ambient pressure or temperature. A quadratic response function is fit to each set of calibration gas measurements. The zero offset and response function are linearly interpolated in time to obtain values appropriate to calculate CO_2 mixing ratio from the instrument response.

To flush the tubing, the solenoid valves for the standard gases are open for 2 min prior to measurement, so that 400 cm^3 of standard gas is used per zero check or calibration (2 min flushing, 2 min measurement). The lifetime of the lowest standard used for zero checking is more than half a year, while the other standards may last as long as 3 years. The standards are calibrated before shipping to Hungary and after their return by CMDL. So far, no significant drift has been observed. The CO_2 standards prepared by CMDL have been found to be very stable over time, so separate working standards are not needed [*Kitzis and Zhao,* 1999].

The off-line postprocessing of the profile data consists of the calculation of the response functions for the CO_2 analyzer and the conversion of the voltage data into physical units. If the change in the response function causes more than 2 ppm change between two consecutive calibrations, the data for the period is rejected. Such periods are rare and almost always caused by significant change in room temperature. The usual change of the response function is below 0.3 ppm. It should be noted that the drift equally influences all monitoring levels, therefore the relative mixing ratio profile is correct even if the absolute accuracy is temporarily lower than usual. As this type of error is random, the long-term accuracy of the values is close to that of the standards (~0.1 ppm [*Zhao et al.,* 1997b]).

2.3. Temperature, Humidity, Wind and Radiation Measurements

At the highest monitoring level, 115 m above the ground, wind speed (Vaisala WAA15A), wind direction (Vaisala WAV15A), and air temperature/humidity sensors (Vaisala HMP35D) are mounted along with the air sampling tube at the end of a 4.4-m-long instrument arm projecting north. The analog signals of the meteorological sensors are digitized by means of a 12 bit analog to digital (A/D) converter and are transmitted to the data acquisition computer via an RS232 serial link. Proper shielding of the cables and sensors, as well as the digitalization of the signals, are essential to avoid

the pickup of noise in the long cables, which may be caused by the nearby high-power antennas. Grounding is also important to minimize the possibility of damage from lightning.

The meteorological instrumentation at 82 m above the ground is similar, but a wind direction sensor is not installed there. In April 1997 a sonic anemometer was installed at this level for eddy flux measurements (see section 2.5).

At the 48-m level the flow distortion caused by the large diameter of the tower (7.75 m) has a significant influence on the wind measurements. Therefore two 2.5-m-long instrument arms were mounted on opposite (north and south) sides of the tower. Anemometers were installed on both arms, and a temperature/humidity sensor and air sample inlet tube were mounted only on the north arm. The flow distortion caused by the tower influences both anemometers and can cause wind speed distortion in excess of ±50% of the real wind speed. We corrected the measured wind speeds based on a theoretical laminar flow pattern around a cylindrical body using wind direction information from the 115-m level. Tower-induced Kármán vortices can also distort the average wind vector in the downwind direction, thus only the wind speed value of the anemometer located on the upwind side of the tower is used for the reconstruction of the wind speed value. Figure 4 illustrates the corrected and uncorrected wind speed data for a typical day during near-neutral stability conditions. Compared to a theoretical log linear wind profile [*Webb,* 1970; *Stull,* 1988], the corrected data give considerably lower root-mean-square error than the uncorrected profile and the corrected data exhibit a more realistic wind profile.

For measurements at 10 m above the ground, a mast was erected ~70 m from the transmitter building and tower. Wind speed, temperature, and humidity sensors are the same as the tower instruments. Instruments for radiation measurements are mounted at 2-m height on the mast, including a global solar radiation sensor (Kipp & Zonen model CM2), a radiation balance sensor (REBS model Q*7), and a photosynthetically active radiation sensor (Li-Cor model LI-190SZ quantum sensor). Sensors for soil temperature and soil heat flux (Campbell Scientific model HFT-3) were recently installed near the mast.

Especially in sunny weather, solar heating of the TV tower body may cause overestimates in the air temperature at the 48-m level, when the wind blows from the SW-SE sector. The temperature is corrected on the basis of the assumption that during daytime, unstable atmospheric conditions the mean temperature at 48 m should fit the lapse rate determined by the 10- and 82-m temperature values. On the basis of the Monin-Obukhov similarity, an approximate relationship between the difference in temperature at 10 and 82 m and the deviation of the 48-m temperature from a linear interpolation of temperature with height is

$$t_{48} \cong t_{10} - (t_{10} - t_{48}) \frac{48 - 10}{82 - 10} - 0.3\,(t_{10} - t_{82})\,. \quad (1)$$

The applied procedure preserves the variability of the observed temperature at 48 m while correcting the smoothed mean value during the critical time periods. Figure 5 shows the uncorrected and corrected temperature minus the values calculated from (1) for July 1997. The bias in uncorrected temperature for southerly wind

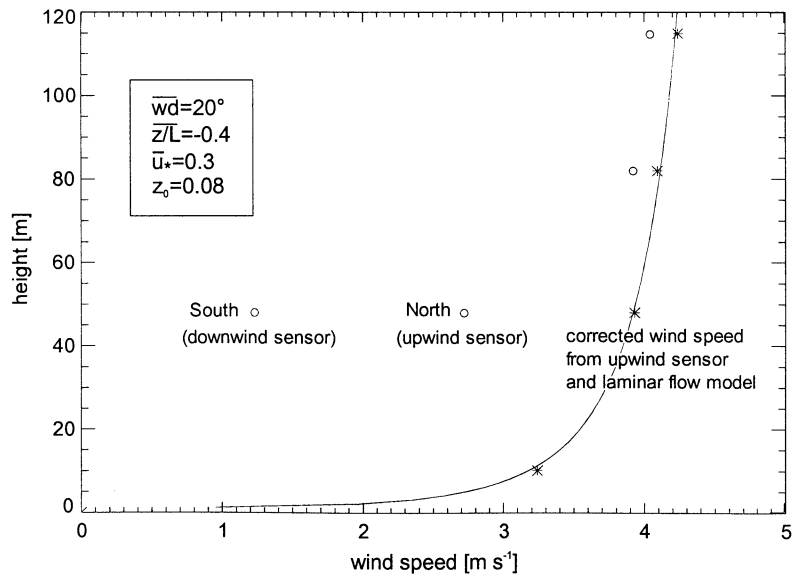

Figure 4. Average wind profiles of uncorrected (circles) and corrected (stars) wind speed data on August 12, 1997, between 0700 and 1400 LST. The average wind direction was 20°. The average 48 m level wind speed data from the upwind and downwind sensors are shown along with the corrected wind speed for that level using the upwind sensor data and laminar flow model.

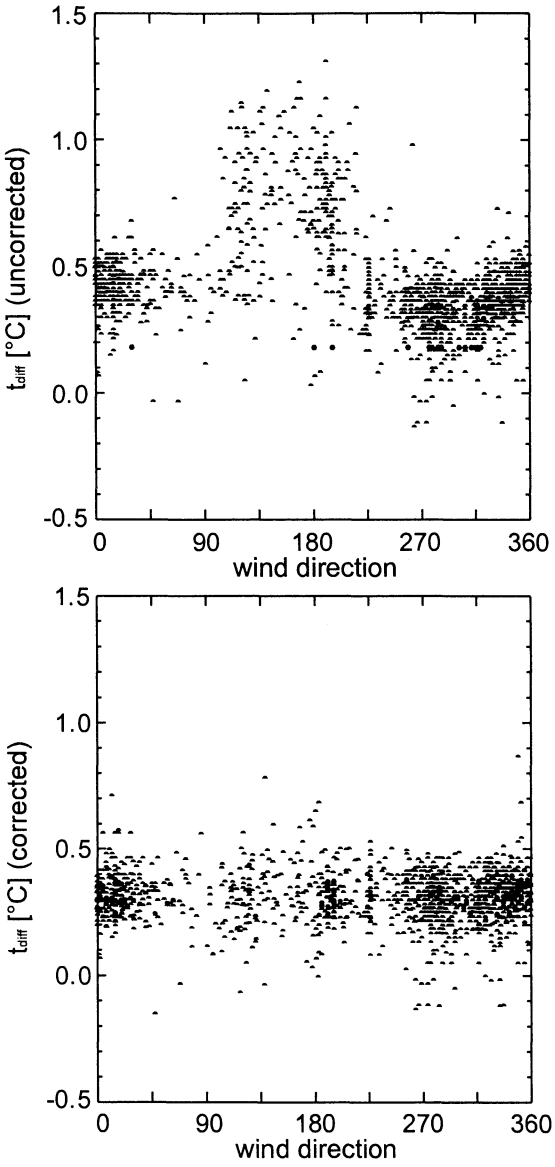

Figure 5. The result of the temperature correction for July 1997 showing (top) uncorrected and (bottom) corrected data (see text for details).

directions is obvious from Figure 5 (top). As expected, the correction has no effect for noncritical wind directions. The humidity sensor measures the relative humidity for the actual environmental condition of the sensor, therefore the measured (uncorrected) temperature is used for calculation of the absolute humidity.

2.4. Data Acquisition and Control

For data acquisition and system control for the CO_2 profiles and meteorological data we use a 286 PC with 1 Mb RAM and a 40 Mb hard disk. The analog signals of the CO_2 analyzer and mass flow controller are read by a multiplexer A/D converter (PCL-711B). The data acquisition and system control software is written in Turbo Pascal (Borland) and runs under DOS 5.0 (Microsoft). During the data integration period the computer consecutively reads data from the meteorological sensors at each monitoring level through its serial port (RS232), then it reads the CO_2 analyzer and the mass flow controller through the PCL-711B card. The profile system generates 5 Mb/month of data, which are stored on a floppy diskette after compression. The data are mailed or carried to our laboratory in Budapest for processing.

2.5. Monitoring System for the Vertical Flux of Carbon Dioxide

Measurements of the vertical flux of CO_2 and H_2O by eddy covariance 82 m above the ground began in April 1997. This was facilitated by mounting to the 4.4-m-long instrument arm an ultrasonic anemometer (Gill Solent Enhanced), an aspirated thermocouple (50 cm from the anemometer) for fast-response temperature measurements, and an additional air sampling tube for CO_2 and H_2O measurements.

A schematic diagram of the air sampling system used to determine the CO_2 and H_2O mixing ratios for flux calculations is shown in Figure 6. Measurements of CO_2 and H_2O are made at 4 Hz using a fast-response

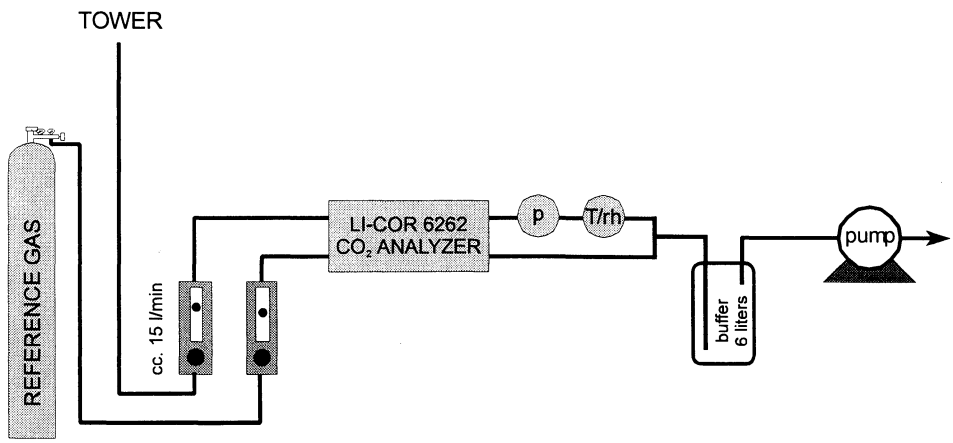

Figure 6. Layout of the system for the vertical CO_2 flux monitoring.

IRGA (Li-Cor model LI-6262). Air is pumped (dual-diaphragm Gast model DAA V175 ED, MFG Corporation) through the sampling tube and analyzer at ~15 L/min, producing a pressure drop of ~45 kPa. Pressure fluctuations generated by the pump are damped by means of a 6-L buffer volume. Flow in the sampling tube is turbulent. Immediately behind the sample cell of the analyzer, we measure pressure (MKS Instruments model 122A barotron), temperature, and relative humidity (Vaisala HMD20YB). The pressure and temperature data are used to correct the instrument response for variations in these parameters (see below). The humidity data are used to determine the calibration function for water vapor measurements by the Li-Cor 6262.

The CO_2 analyzer runs in relative mode. Dry, synthetic air with a CO_2 mixing ratio of 330-340 ppm is used as a reference gas (Messer Hungarogáz) and flows at a rate of 5-10 cm^3/min through the reference cell of the IRGA. The analog output of the analyzer for CO_2 and H_2O, as well as the signals of the pressure and temperature/humidity sensors, are digitalized by the common A/D RS232 converter.

A separate data acquisition computer (486 PC with a 40 MHz CPU, 4 Mb RAM, 1 Gb HD) is used to read data from the fast-response instruments (sonic anemometer, thermocouple, and IRGA). The computer communicates with the instruments through two standard serial ports: COM1 receives the data from the sonic anemometer, while the two A/D RS232 devices are controlled via COM2. The data acquisition cycle is triggered by the signal from the sonic anemometer. After reception of a data package (horizontal and vertical wind speed, wind direction, and error code) the computer requests data from the aspirated thermocouple, the CO_2/H_2O analyzer and its accessory sensors (pressure, temperature/humidity), and the CO_2 profile analyzer. The position of the multiport valve of the profile system is also determined. As the time of the change of the position of the multiport valve is recorded on the computers of both the profile and eddy correlation systems, the parallel records allow the synchronization of the two independent data acquisition computers. The data acquisition software is written in Turbo Pascal language and runs under DOS 5.0. The eddy correlation system produces data at a rate of ~600 Mb/month, and the data are stored on a CD-R without compression.

The response of the IRGA is calibrated by comparison to ambient CO_2 and H_2O measurements from the slow-response sensors, similar to the method of *Berger et al.* [2000]. A calibrated CO_2 measurement is typically obtained every 8 min at the 82-m level. Exact synchronization of the signals requires accounting for the time for air to pass through the sampling tubes of the profile and eddy flux systems. The lag time of the profile system is calculated from the measured flow rates. For the eddy correlation system, two different lag time values are calculated for H_2O and CO_2 [*Moncrieff et al.,* 1997] as a daily average of 10 individual lag time tests using a spectral method. First, the daily lag time values are calculated without any restrictions for the whole data set. Then a polynomial is fitted to the long-term lag time series, which is used to determine the actual lag time window where the maximum correlation is supposed to occur during a specific day. The time window used is 12 s around the fitted value. The daily lag time values calculated from the second run are used for the synchronization and later for the calculation of lagged covariances.

For calibration of the H_2O and CO_2 response of the IRGA we use the following function:

$$f\left(V\frac{p_0}{p}\right)\frac{T}{T_0} + C_r = C\,, \tag{2}$$

where V is the voltage signal of the analyzer, p_0 is the reference pressure (1000 hPa), p is the pressure in the measuring cell, C_r is the mole fraction of CO_2 or H_2O in the reference gas (zero for H_2O, 330-340 μmol/mol for CO_2), T_0 is the reference temperature (273.15 K), T is the temperature in the measuring cell, and C is the mole fraction of H_2O or CO_2 measured by the calibrated instruments. The analyzer is calibrated in terms of H_2O and CO_2 mole fraction [*McDermitt et al.,* 1993]. Linear regression is carried out between $(C - C_r)(T_0/T)$ and $V(p_0/p)$ to determine the slope of the response function, f. Figure 7 shows the fit for a typical day. Occasional outliers are removed interactively, and the resulting linear fits typically show very high correlation. The manufacturer provides a fifth-order polynomial calibration curve for the instrument, but the polynomial differs only slightly from linear in the range of interest (360-500 ppm) as shown by the inset in Figure 7. Calibration values are determined for each 24 hours of measurement. The calibration factors are quite stable in time. Since the fluctuations of H_2O and CO_2 measured by the Li-Cor 6262 are expressed in terms of mole fraction relative to dry air, it is not necessary to perform the corrections for variations of the density of air [e.g., *Webb et al.,* 1980; *Grelle and Lindroth,* 1996].

Three-dimensional wind vector rotation is applied to the sonic anemometer data following the method of *Lee* [1998]. Rotation angles and measured average vertical wind speed are calculated and stored for each hourly period.

A linear trend is removed from each 60-min interval of all data used for eddy flux calculations (wind components, temperature, H_2O, and CO_2). Data values outside $\pm 4\sigma$ are removed. Turbulent fluxes are calculated from covariances of the detrended time series taking into account the delay time of signals determined during the calibration procedure outlined above.

Spectral corrections are applied in order to account for the damping of fluctuations caused by the long air sample tubes, limited sensor response time, sensor line averaging and sensor separation, and sampling [*Moore,*

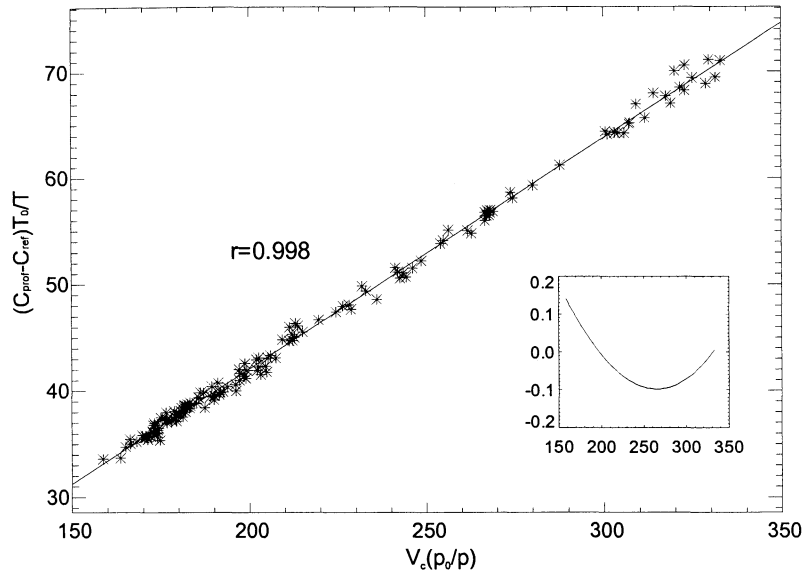

Figure 7. Linear calibration approximation for CO_2 on June 17, 1997. Inset shows the difference between the fifth-order polynomial supplied by the IRGA manufacturer and the linear approximation.

1986; *Leuning and Moncrieff,* 1990; *Lenschow and Raupach,* 1991; *Massman,* 1991]. The scheme of *Moore* [1986] is applied through the use of transfer functions for each correction term. Corrections are based on the modified forms of model spectra of *Kaimal et al.* [1972] [*Moore,* 1986; *Moncrieff et al.,* 1997]. The transfer function method is based on the assumption of spectral similarity between temperature, H_2O, and CO_2 [*Anderson and Verma,* 1984; *Ohtaki,* 1985]. Average losses of the eddy correlation system calculated from the theoretical considerations are ~10% for CO_2 and ~9% for H_2O. It appears that the water vapor signal suffers from excess spectral degradation compared with the theoretical spectral damping because of the long tubing of the system, which causes extra loss of water vapor flux. This effect needs more investigation, but this is out of scope of this paper.

To determine the quality of the measurement and to classify the data, *Foken and Wichura* [1996] propose three tests: the instationarity test, the correlation test, and the integral turbulent characteristics test. We apply the instationarity test to the hourly flux values. The quality flags (e.g., the percentage of instationarity) can be used in the determination of the net carbon balance of the region in such a way that flux values beyond a specific threshold instationarity are not used, resulting in less random error in the measurement. However, it should be noted that the effect of random error in the determination of the net carbon budget of the region is not severe if the time series available is long enough [*Moncrieff et al.,* 1996].

3. Results

In this paper we present only a few examples illustrating the measurements. Detailed evaluation and interpretation of the data will be published separately. *Haszpra* [1999] presents time series and average vertical gradients of CO_2 mixing ratios at the site and a comparison of CO_2 data from the Hegyhátsál tower with data from the World Meteorological Organization (WMO) Global Atmosphere Watch (GAW) K-puszta site in central Hungary.

The weekly flask samples collected for analysis by CMDL provide an independent check on the calibration of our CO_2 mixing ratio measurements. The relationship between flask measurements and simultaneous in situ data (with a few outliers rejected) does not differ significantly from 1:1 (slope = 0.945, residual standard deviation = 2.2 ppm, number of samples = 104, data not shown). The large relative standard deviation (RSD) reflects the high degree of temporal variability of CO_2 mixing ratios at our site and the difficulty of matching the flask and in situ data exactly in time. (The flask data are available on the Internet via anonymous FTP to ftp.cmdl.noaa.gov; paths: /ccg/co2/flask/complete/hun.co2).

Figure 8 and Figure 9 present the vertical distribution of the CO_2 mixing ratio during typical winter and summer weeks, respectively. In winter the surface is only a source of CO_2 due to respiration and anthropogenic emissions, and the mixing ratio gradient is always negative (i.e., more CO_2 nearer the surface). The strength of the wintertime gradient is mainly a reflection of the vigor of vertical air mixing. During periods of high stability the gradient between 10 and 115 m can be many tens of ppm. The gradual increase of CO_2 during the period presented in Figure 8 resulted from an accumulation process that is caused by pooling of cold air in the Carpathian Basin during stagnant weather conditions. Such conditions often persist for many days in winter.

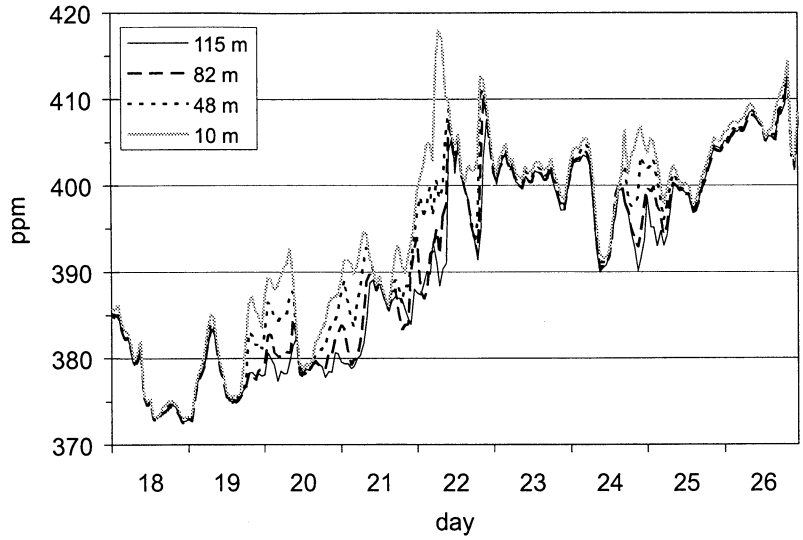

Figure 8. Temporal variation of the vertical distribution of CO_2 mixing ratio during a week in winter (November 18-26, 1997).

In summer, as shown in Figure 9, the biogenic fluxes (photosynthesis and respiration) are large and lead to a large diurnal variation of CO_2 near the ground. Net photosynthesis during the daytime is coincident with vigorous convective mixing of the air in the planetary boundary layer that results in positive daytime gradients which are generally small in magnitude, averaging a few tenths of ppm between 10 and 115 m during July afternoons (lower CO_2 at 10 m than 115 m). Stable stratification of the atmosphere at night results in extremely high mixing ratios near the surface and very large negative gradients. On many nights the stratification is so strong and shallow that accumulation of CO_2 is confined to the region below the 48 m level (e.g., August 24-25).

Our observations of CO_2 mixing ratio vertical profiles cover a longer period than the direct flux measurements, and the profile measurement system is more reliable in general. Hence it would be useful to be able to calculate surface fluxes from the profile data, at least for some periods. Estimates of the vertical mass transport of CO_2 and other scalars can be obtained by using surface layer similarity theory (which describes surface layer flux-gradient relationships [e.g., see *Businger et al.*, 1971; *Foken and Skeib,* 1983; *Businger,* 1986; *Stull,* 1988; *Yagüe and Cano,* 1994; *Saigusa et al.,* 1996; *Hensen et al.,* 1997]), if the vertical profiles of the wind speed and air temperature are also available [see *Stull,* 1988, chapter 6]. We have chosen the revised similarity functions of *Högström* [1996, equations (5)-(8)] for our purposes. The calculations can then be verified against measured fluxes. Applicability of the similarity theory has several preconditions (see *Foken and Wichura* [1996] for a detailed overview). In our case the unusually large

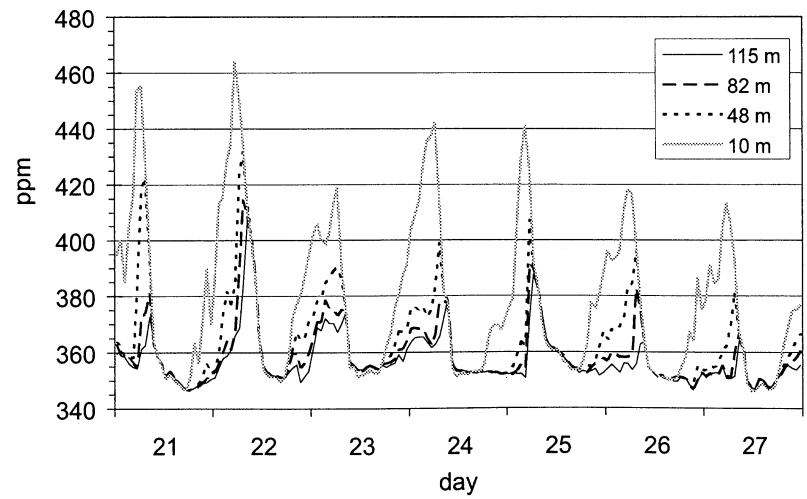

Figure 9. Temporal variation of the vertical distribution of CO_2 mixing ratio during a week in summer (August 21-27, 1996).

height differences between the measuring levels cause additional uncertainty in the estimation of the similarity profiles but also contribute to improved estimates of the (often small) mixing ratio gradients. Difficulty arises during nighttime stable conditions when we are restricted to using data measured by the two lowest levels (10 and 48 m) for the estimation of fluxes to ensure that the utilized data reside in the surface layer [*Stull,* 1988; *Yagüe and Cano,* 1994]. During unstable conditions we use data of the three lowest levels, up to 82-m height. At night the 82-m level is often above the inversion layer, and so it is completely decoupled from the ground.

Direct comparison of surface fluxes computed from flux-gradient relationships and by using eddy covariance is complicated for nonhomogeneous surfaces because the region of the surface ("footprint" [*Schmid,* 1994, 1997]) influencing each estimation may be different. *Horst* [1999] shows that the source areas associated with fluxes measured by application of similarity theory and the eddy correlation technique should be approximately equal if the eddy correlation measurement is made at the "effective measuring height," which is defined as the arithmetic mean of the elevations of the highest and lowest profile measurements for stable stratification or the geometric mean for unstable stratification [*Horst,* 1999]. In our case the effective measuring height is 28.6 m during daytime and 29 m during nighttime. Thus, compared with eddy correlation measurements at 82 m, the two methods for flux determination always represent different source areas in the mosaic-type terrain (see Figure 2). This may cause differences between the calculated fluxes. Furthermore, fluxes determined by eddy correlation are expected to be reliable even during slightly nonsteady conditions, whereas the validity of the flux-profile relationship is questionable for such conditions. Computational problems occur during highly stable conditions owing to the failure of convergence in the iterative calculation method using the flux-profile relationship causing lack of flux data during many nights. Intermittent turbulence at night also causes uncertainties. The error correction routines outlined above are also a possible source of error because of the uncertainties in the temperature reconstruction routine.

The net ecosystem exchange (NEE) (the sum of the eddy flux at 82 m, and the rate of change of CO_2 storage below 82 m) calculated from the eddy correlation technique can be used to estimate the error term in the similarity theory calculations. It should be noted that there are also large uncertainties associated with the eddy correlation technique [e.g., *Moncrieff et al.,* 1996], yet this method is the most accurate to date. The accuracy of the NEE calculation is improved with a more precise storage term calculation (see below).

In our case the mean daily cycle of the deviation of the profile fluxes from NEE is calculated for each month using the data from all available years. The data comparison shows that there is a systematic underestimation of NEE calculated from the profile method during daytime and a smaller systematic overestimation during nighttime. There is an emphasized underestimation during the morning transition period. Construction of a new, site-specific similarity function for CO_2 based on the existing NEE data, following the method of, e.g., *Högström* [1988], gave better results, but the problem of the morning transition period was not solved. This problem can be eliminated if the calculated monthly average daily deviations are simply added to the daily profile CO_2 flux data calculated from the similarity theory.

Figure 10 compares the NEE calculated from the profile data by means of the surface layer similarity theory and from the direct flux measurements by means of the eddy correlation technique for a continuous 7-day period. The figure shows the raw, unmodified profile fluxes (dotted line) versus NEE (solid line) and the modified similarity fluxes (dashed line). The matching of the data is significantly improved with the new method applied.

Similarity theory also provides a good framework for the NEE calculations in another way. The NEE calculations need precise carbon dioxide storage calculations [*Fan et al.,* 1990] from the concentration profiles. A

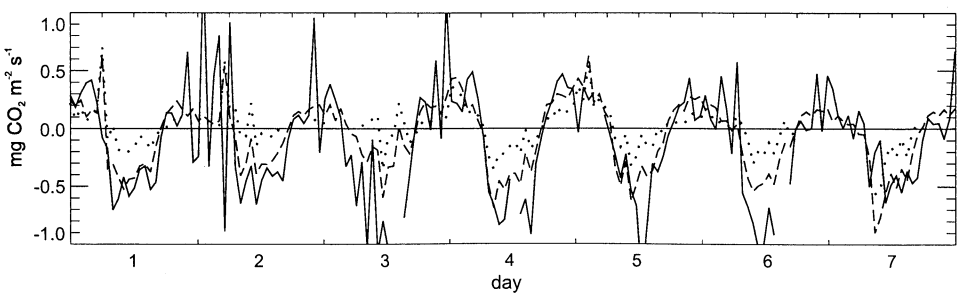

Figure 10. Comparison of fluxes measured by the two methods and the effect of the correction on the profile method (see text). Solid line, net ecosystem exchange (eddy CO_2 flux plus rate of change of storage); dotted line, original, unmodified profile CO_2 flux; dashed line, modified profile CO_2 flux.

more accurate storage calculation is performed by fitting the concentration data to obtain the concentration profile using an appropriate similarity function compared to profiles calculated using simple linear interpolation between levels.

4. Conclusions

We have described an ongoing program being carried out in Hungary to investigate the role of the temperate continental region in the global carbon cycle. In summary, flux estimates based solely on theoretical flux-profile relationships from similarity theory do not provide accurate, long-term carbon budget estimates because of both random and systematic errors and site-specific factors. Since selective systematic errors can change even the sign of the long-term net carbon dioxide budget of a region [*Moncrieff et al.,* 1996], these errors can cause significant bias in the overall regional net source/sink estimation. In spite of these weaknesses of the profile flux data set, it is useful for filling the data gaps that inevitably occur during long-term eddy correlation measurements.

The data measured at Hegyhátsál are available from the lead author on request. The profile data are also incorporated into the GLOBALVIEW-CO_2 database (available via anonymous FTP to ftp.cmdl.noaa.gov; path: /ccg/co2/GLOBALVIEW).

Acknowledgments. Use of the tower and transmitter building was kindly provided by Antenna Hungária Corporation. The project was supported by the U.S.-Hungarian Scientific and Technological Joint Fund [J.F. 162 (1992-1995) and J.F. 504 (1996-1999)] and by the Hungarian National Scientific Research Fund [OTKA T7282 (1993-1996), OTKA T23811 (1997-2000) and OTKA T32440 (2000-2003)]. The authors thank F. Nerada, technician from the Institute for Atmospheric Physics, who constructed and mounted most parts of the measuring system, and Z. Nagy (Hungarian Meteorological Service) and J. Nagy (HWI, Hungary) for coding the data acquisition software and for designing, producing, and installing the A/D RS232 converters, as well as J. Szabó (Research Institute for Soil Science and Agricultural Chemistry) for his contribution to the site description. The authors appreciate the valuable advice of Zs. Iványi (Eötvös Loránd University), and they especially thank P. Tans (NOAA CMDL) for the inspiration for the whole project.

References

Anderson, D. E., and S. B. Verma, Turbulence spectra of CO_2, water vapor, temperature and wind velocity fluctuations over a crop surface, *Boundary Layer Meteorol. 33,* 1-14, 1984.

Bakwin, P. S., P. P. Tans, C. L. Zhao, W. Ussler III, and E. Quesnell, Measurements of carbon dioxide on a very tall tower, *Tellus, Ser. B, 47,* 535-549, 1995.

Bakwin, P.S., P. P. Tans, D.F. Hurst, and C. Zhao, Measurements of carbon dioxide on very tall towers: Results of the NOAA/CMDL program, *Tellus, Ser. B, 50,* 401-415, 1998.

Baldocchi, D., R. Valentini, S. Running, W. Oechel, and R. Dahlman, Strategies for measuring and modelling carbon dioxide and water vapour fluxes over terrestrial ecosystems, *Global Change Biol. 2,* 159-168, 1996.

Barnola, J. M., M. Anklin, J. Porcheron, D. Raynaud, J. Schwander, and B. Stauffer, CO_2 evolution during the last millennium as recorded by Antarctic and Greenland ice, *Tellus, Ser. B, 47,* 264-272, 1995.

Berger, B.W., K.J. Davis, P.S. Bakwin, C. Yi, and C. Zhao, Long-term carbon dioxide fluxes from a very tall tower in a northern forest: Flux measurement methodology, *J. Atmos. Oceanic. Technol., in press,* 2000.

Businger, J. A., Evaluation of the accuracy with which dry deposition can be measured with current micrometeorological techniques, *J. Clim. and Appl. Meteorol., 25,* 1100-1124, 1986.

Businger, J. A., J. C., Wyngaard, Y. Izumi, and E. F. Bradley, Flux-profile relationships in the atmospheric surface layer, *J. Atmos. Sci. 28,* 181-189, 1971.

Ciais, P., P. P. Tans, M. Trolier, J. W. C. White, and R. J. Francey, A large northern hemispheric terrestrial CO_2 sink indicated by the $^{13}C/^{12}C$ ratio of atmospheric CO_2, *Science 269,* 1098-1102, 1995a.

Ciais, P., P. P. Tans, J. W. C. White, M. Trolier, R. J. Francey, J. A. Berry, D. R. Randall, P. J. Sellers, J. G. Collatz, and D. S. Schimel, Partitioning of ocean and land uptake of CO_2 as inferred by ^{13}C measurements from the NOAA/CMDL global air sampling network, *J. Geophys. Res., 100,* 5051-5070, 1995b.

Conway, T. J., P. P. Tans, L. S. Waterman, K. W. Thoning, D. R. Kitzis, K. A. Masarie, and N. Zhang, Evidence for interannual variability of the carbon cycle from the National Oceanic and Atmospheric Administration/Climate Monitoring and Diagnostics Laboratory Global Air Sampling Network, *J. Geophys. Res., 99,* 22,831-22,855, 1994.

Denning, A. S., I. Y. Fung, and D. Randall, Latitudinal gradient of atmospheric CO_2 due to seasonal exchange with land biota, *Nature, 376,* 240-243, 1995.

Dixon, R. K., S. Brown, R. A. Houghton, A. M. Solomon, M. C. Trexler, and J. Wisniewski, Carbon pools and flux of global forest ecosystems, *Science, 263,* 185-190, 1994.

Enting, I. G., and J. V. Mansbridge, Latitudinal distribution of sources and sinks of CO_2: Results of an inversion study, *Tellus, Ser. B, 43,* 156-170, 1991.

Etheridge, D. M., L. P. Steele, R. L. Langenfelds, R. J. Francey, J. M. Barnola, and V. I. Morgan, Natural and anthropogenic changes in atmospheric CO_2 over the last 1000 years from air in Antarctic ice and firn, *J. Geophys. Res., 101,* 4115-4128, 1996.

Fan, S. M., S. C. Wofsy, P.S. Bakwin, D. J. Jacob, and D.R. Fitzjarrald, Atmosphere-biosphere exchange of CO_2 and O_3 in the central Amazon Forest, *J. Geophys. Res., 95,* 16,851-16,864, 1990.

Foken, T., and G. Skeib, Profile measurements in the atmospheric near-surface layer and the use of suitable universal function for the determination of the turbulent energy exchange, *Boundary Layer Meteorol., 25,* 55-62, 1983.

Foken, T., and B. Wichura, Tools for quality assessment of surface-based flux measurements, *Agric. For. Meteorol., 78,* 83-105, 1996.

Grelle, A., and A. Lindroth, Eddy-correlation system for long-term monitoring of fluxes of heat, water vapour and CO_2, *Global Change Biol., 2,* 297-307, 1996.

Haszpra, L., On the representativeness of carbon dioxide measurements, *J. Geophys. Res., 104,* 26,953-26,960, 1999.

Hensen, A., W. C. M. van den Bulk, A. T. Vermeulen, and G. P. Wyers, CO_2 exchange between grassland and the atmosphere, *Neth. Energy Res. Found., Rep. ECN-C-97-032,* Petten, 1997.

Hesshaimer, V., M. Heiman, and I. Levin, Radiocarbon evi-

dence for a smaller oceanic carbon dioxide sink than previously believed, *Nature, 370,* 201-203, 1994.

Högström, U., Non-dimensional wind and temperature profiles in the atmospheric surface layer: A re-evaluation, *Boundary Layer Meteorol., 42,* 55-78, 1988.

Högström, U., Review of some basic characteristics of the atmospheric surface layer, *Boundary Layer Meteorol., 78,* 215-246, 1996.

Horst, T. W., The footprint for estimation of atmosphere-surface exchange fluxes by profile techniques, *Boundary Layer Meteorol., 90,* 171-188, 1999.

Kaimal, J. C., J. C. Wyngaard, Y. Izumi, and O. R. Cote, Spectral characteristics of surface-layer turbulence, *Q. J. R. Meteorol. Soc., 98,* 563-589, 1972.

Keeling, C. D., R. B. Bacastow, A. F. Carter, S. C. Piper, T. P. Whorf, M. Heimann, W. G. Mook, and H. Roelffzon, A three-dimensional model of atmospheric CO_2 transport based on observed winds, 1, Analysis of observational data, in *Aspects of Climate Variability in the Pacific and Western Americas, Geophys. Monogr. Ser.,* vol. 55, edited by D.H. Peterson, pp. 165-236, AGU, Washington, D.C., 1989.

Keeling, R. F., S. C. Piper, and M. Heimann, Global and hemispheric CO_2 sinks deduced from changes in atmospheric O_2 concentration, *Nature, 381,* 218-221, 1996.

Kitzis, D., and C. Zhao, CMDL/Carbon Cycle Gases Group standards preparation and stability, *Tech. Memor. ERL CMDL-14,* Natl. Oceanic and Atmos. Admin., Boulder, Colo., 1999.

Lee, X., On micrometeorological observations of surface-air exchange over tall vegetation, *Agric. and For. Meteorol., 91,* 39-49, 1998.

Lenschow, D. H., and M. R. Raupach, The attenuation of fluctuations in scalar concentrations through sampling tubes, *J. Geophys. Res., 96,* 15,259-15,268, 1991.

Leuning, R., and J. Moncrieff, Eddy-covariance CO_2 flux measurements using open- and closed-path CO_2 analysers: Corrections for analyser water vapour sensitivity and damping of fluctuations in air sampling tubes, *Boundary Layer Meteorol., 53,* 63-76, 1990.

Massman, W. J., The attenuation of concentration fluctuations in turbulent flow through a tube, *J. Geophys. Res., 96,* 15,269-15,273, 1991.

McDermitt, D. K., J. M. Welles, and R. D. Eckles, Effects of temperature, pressure and water vapor on gas phase infrared absorption by CO_2, *LI-COR Tech. Publ., 116,* Lincoln, Nebraska, 1993.

Moncrieff, J. B., Y. Malhi, and R. Leuning, The propagation of errors in long-term measure-ments of land-atmosphere fluxes of carbon and water, *Global Change Biol., 2,* 231-240, 1996.

Moncrieff, J. B., J. M. Massheder, H. de Bruin, J. Elberts, T. Friborg, B. Heusinkveld, P. Kabat, P. Scott, H. Soegaard, and A. Verhoef, A system to measure surface fluxes of momentum, sensible heat, water vapour and carbon dioxide, *J. Hydrol., 188-189,* 589-611, 1997.

Moore, C. J., Frequency response corrections for eddy correlation systems, *Boundary Layer Meteorol., 37,* 17-35, 1986.

Musselman, R. C., and D. G. Fox, A review of the role of temperate forests in the global CO_2 balance, *J. Air Waste Manage. Assoc., 41,* 798-807, 1991.

Ohtaki, E., On the similarity in atmospheric fluctuations of carbon dioxide, water vapor and temperature over vegetated fields, *Boundary Layer Meteorol., 32,* 25-37, 1985.

Quay, P. D., B. Tilbrook, and C. S. Wong, Oceanic uptake of fossil fuel CO_2: Carbon-13 evidence, *Science, 256,* 74-79, 1992.

Saigusa, N., S. Liu, T. Oikawa, and T. Watanabe, Seasonal change in CO_2 and H_2O exchange between grassland and atmosphere, *Ann. Geophys., 14,* 342-350, 1996.

Sarmiento, J. L., and E. T. Sundquist, Revised budget for the oceanic uptake of anthropogenic carbon dioxide, *Nature, 356,* 589-593, 1992.

Schmid, H. P., Source areas for scalars and scalar fluxes, *Boundary Layer Meteorol., 67,* 293-318, 1994.

Schmid, H. P., Experimental design for flux measurements: Matching scales of observations and fluxes, *Agric. For. Meteorol., 87,* 179-200, 1997.

Siegenthaler, U., and J. L. Sarmiento, Atmospheric carbon dioxide and the ocean, *Nature, 365,* 119-125, 1993.

Stefanovits, P., Brown Forest Soils of Hungary, *Akad. Kiadó,* Budapest, 1971.

Stull, R. B., *An Introduction to Boundary Layer Meteorology,* Kluwer Acad., Norwell, Mass., 1988.

Sundquist, E. T., The global carbon dioxide budget, *Science, 259,* 934-941, 1993.

Taguchi, S., A three-dimensional model of atmospheric CO_2 transport based on analyzed winds: Model description and simulation results for TRANSCOM, *J. Geophys. Res., 101,* 15,099-15,109, 1996.

Tans, P. P., An observational strategy for assessing the role of terrestrial ecosystems in the global carbon cycle: Scaling down to regional levels, in *Scaling Processes Between Leaf and Landscape Levels,* edited by J. Ehleringer and C. Field, Academic, San Diego, Calif., 71-105, 1991.

Tans, P. P., T. J. Conway, and T. Nakazawa, Latitudinal distribution of the sources and sinks of atmospheric carbon dioxide derived from surface observations and an atmospheric transport model, *J. Geophys. Res., 94,* 5151-5172, 1989.

Tans, P. P., I. Y. Fung, and T. Takahashi, Observational constrains on the global atmospheric CO_2 budget, *Science, 247,* 1431-1438, 1990.

Tans, P. P., P. S. Bakwin, and D. W. Guenther, A feasible Global Carbon Observing System: A plan to decipher today's carbon cycle based on observations, *Global Change Biology 2,* 309-318, 1996.

Trenberth, K. E., J. T. Houghton, and L. G. Meira Filho, The Climate System: An overview, in *Climate Change 1995, The Science of Climate Change,* edited by J.T. Houghton et al., pp 51-64, Cambridge Univ. Press, New York, 1996.

Trolier, M., J. W. C. White, P.P. Tans, K.A. Masarie, and P.A. Gemery, Monitoring the isotopic composition of atmospheric CO_2: Measurements from the NOAA global air sampling network, *J. Geophys. Res.,* J. *101,* 25,897-25,916, 1996.

Valentini, R., J. A. Gamon, and C. B. Field, Ecosystem gas exchange in a California grassland: Seasonal patterns and implications for scaling, *Ecology, 76,* 1940-1952, 1995.

Webb, E. K., Profile relationships: The log-linear range, and extension to strong stability, *Q. J. R. Meteorol. Soc., 96,* 67-90, 1970.

Webb, E. K., G. I. Pearman, and R. Leuning, Correction of flux measurements for density effects due to heat and water vapour transfer, *Q. J. R. Meteorol. Soc., 106,* 85-100, 1980.

Yagüe, C., and J. L. Cano, Eddy transfer processes in the atmospheric boundary layer, *Atmos. Environ., 28,* 1275-1289, 1994.

Zhao, C. L., P. S. Bakwin, and P.P. Tans, A design for unattended monitoring of carbon dioxide on a very tall tower, *J. Atmos. Oceanic Technol., 14,* 1139-1145, 1997a.

Zhao, C. L., P. P. Tans, and K. W. Thoning, A high precision manometric system for absolute calibration of CO_2 in dry air, *J. Geophys. Res., 102,* 5885-5894, 1997b.

P. S. Bakwin, Climate Monitoring and Diagnostics Laboratory, NOAA, 325 Broadway, Boulder, CO 80303. (pbakwin@cmdl.noaa.gov)

Z. Barcza and T. Weidinger, Department of Meteorology, Eötvös Loránd University, P.O.Box 32, H-1518 Budapest, Hungary. (bzoli@elte.hu; weidi@ludens.elte.hu)

B. W. Berger and K. J. Davis, Department of Soil, Water and Climate, University of Minnesota, 1991 Upper Buford Circle, St. Paul, MN 55108-6028. (bberger@gis.umn.edu; kdavis@soils.umn.edu)

L. Haszpra, Institute for Atmospheric Physics, Hungarian Meteorological Service, P.O.Box 39, H-1675 Budapest, Hungary. (haszpra.l@met.hu)

(Received June 16, 2000; revised August 29, 2000; accepted September 15, 2000.)